SB^{3}C2015
Summer Biomechanics, Bioengineering and Biotransport Conference
June 17-20, 2015,Snowbird Resort, Utah, USA

IN VITRO AND COMPUTATIONAL FLUID DYNAMICS COMPARISON OF THE FLOW DIVERSION EFFICACY OF FIVE COMMERCIAL STENTS

Ronak J. Dholakia (1), Andrew Pagano (1), Fotis Drakopoulos (2), Ari Kappel (1), Chander Sadasivan (1), Xiangmin Jiao (3), David J. Fiorella (1), Nikos Chrisochoides (2), Henry H. Woo (1), Baruch B. Lieber (1)

(1) Department of Neurological Surgery
Stony Brook University
Stony Brook, NY, USA

(2) Department of Computer Science
Old Dominion University
Norfolk, VA, USA

(3) Department of Applied Mathematics and Statistics
Stony Brook University
Stony Brook, NY, USA

INTRODUCTION

Brain aneurysms are abnormal ballooning of intracranial arteries which when left untreated may result in fatal outcome for the patients. Neurovascular stents have been used extensively in stent-assisted coiling treatment of aneurysms. Treatment with flow diverters (low porosity, fine-mesh stents) is used for complicated aneurysm geometries not amenable to coiling. Angiographic analysis with mathematical modeling has been applied for comparison of different flow diversion designs as well as towards prediction of flow diversion efficacy [1]. High resolution computational fluid dynamics (CFD) simulations would provide the opportunity to study localized alterations in hemodynamics due to different devices. Current class of CFD studies with flow diverters in cerebral aneurysm models do not use realistic wire configurations in their models and the fine differences in porosity and pore density across the aneurysm neck might produce inaccurate results. The proposed study aims to test five commercially available neurovascular devices that have not been compared before through angiographic washout analysis and accurate microCT-based mesh reconstruction and CFD analysis in idealized sidewall aneurysm models.

METHODS

Five identical silicone elastomer replicas of an idealized geometry (Figure 1) were manufactured by dip coating. Parent artery diameter of the model was selected to be 4 mm and aneurysm diameter of 7 mm. Briefly, the geometry was printed with a rapid prototyper, the printed core was dipped in solvents to reduce surface roughness and then coated evenly with silicone using an in-house multi-axis spinner. After curing of the silicone, the core was dissolved to obtain a compliant luminal replica of the geometry. Five commercially available neurovascular stents including Pipeline (Covidien Medtronic), FRED, LVIS (Microvention Terumo), Enterprise (Codman J&J), and Neuroform (Boston Scientific Stryker) were implanted in idealized sidewall aneurysm silicone models (Figure 1).

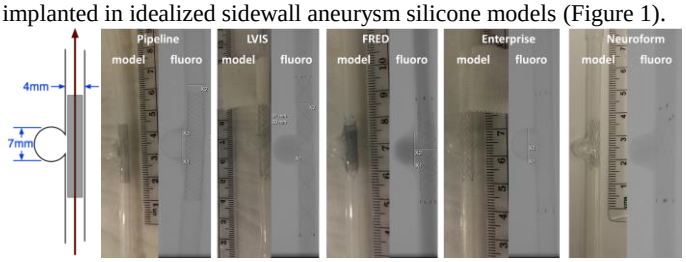

FIGURE 1: SCHEMATIC OF THE IDEALIZED SIDEWALL ANEURYSM MODEL (LEFT) AND CAMERA AND FLUOROSCOPIC SHOTS OF THE FIVE DEVICES IMPLANTED IN SILICONE MODELS

High speed angiographic washout data was acquired in all models at 15 frames/sec under steady flow through a peristaltic pump at approximately 3.5 ml/sec. As a blood replica, 50% glycerol solution was used to obtain a fluid with viscosity of 4cP at a temperature 37C. The silicone model was fit in position in the flow loop and kept immobile while acquiring the images. A 4 French injection catheter was positioned such that the catheter tip was about 50 cm away from the region of interest leaving sufficient length for contrast mixing with the working fluid. Contrast was injected through a power injector at 2.5 ml/sec for 2 seconds with a 2 second delay in injections to allow the C-arm to acquire the mask for the angiogram. Angiographic runs were acquired for a total of 6 times through each model (3 with the inlet and outlet reversed) to ensure repeatability of the data.

The aneurysm region of interest was segmented in the angiographic images to calculate the total gray scale intensity at every

point in time and thus the contrast concentration-time or washout curves (Figure 2) were acquired. The contrast concentration-time curves (washout curves) within the aneurysm were then fitted using a least square approach to a previously developed mathematical model [1] that differentiates convective and diffusive flow regimes within the aneurysm.

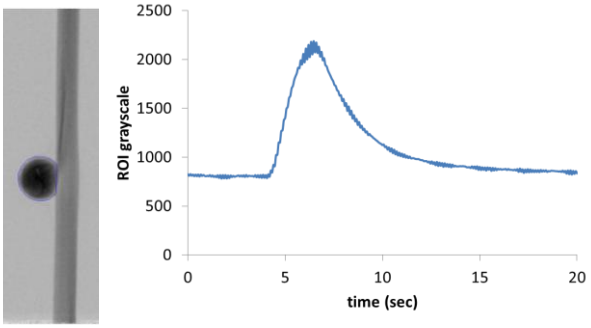

FIGURE 2: SEGMENTED ANEURYSM REGION OF INTEREST (ROI) AND CORRESPONDING CONTRAST CONCENTRATION-TIME CURVE

To obtain the exact implanted position inside the silicone model as well as geometry of the devices, the models were imaged with microCT (uCT50 Scanco Medical, Bruttisellen, Switzerland). All models except FRED were scanned at a resolution of 12microns except FRED at 6microns.

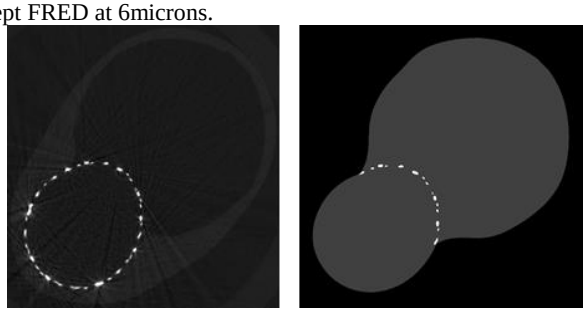

FIGURE 3: RAW MICROCT SLICE FOR PIPELINE MODEL (LEFT) AND AFTER SEGMENTATION WITH THE DEVICE WIRES CROPPED (RIGHT)

Mimics (Materialise, Leuven, Belgium) software is used to perform image segmentation on the microCT data. Two different labels are tagged to the lumen of the sidewall aneurysm model and the flow diverter. During segmentation the device is cropped to only retain the portion providing neck coverage of the aneurysm (Figure 3).

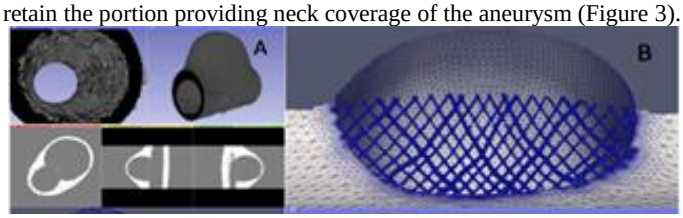

FIGURE 4: ASSEMBLY OF THE 3D OBJECT FROM 2D AXIAL SLICES (A), AND GRADATION AND THE SMOOTHNESS OF THE MESH (B)

We use an automatic and high fidelity image-to-mesh (I2M) conversion scheme that involves combination of the axial image slices using Insight toolkit's (ITK) tile image filter to stack the 2D slices and generate the volume label image that serves as an input for the creation of a Body-Centered Cubic (BCC) which creates a uniform structured BCC lattice by modifying an existing approach [2]. The BCC lattice is refined according to local feature size of labels in the 3D segmented image. The resolution of each labeled object is automatically adjusted based on the user-defined fidelity. Finally, the Mesh Compression step is used to smooth the BCC mesh in order to match the objects' boundaries (Figure 4). The mesh generated as a result is imported in ADINA 9.0 and CFD simulations in the finite element formulation will be run through each computational model.

RESULTS and DISCUSSION

Preliminary angiographic analysis (n=3 each case) indicates reduction in the amplitude of the concentration curves following implantation of the devices. Reduction in amplitude was largest for Pipeline and FRED (Figure 5). Washout parameters obtained following optimization indicate delayed convection (increase in convective time constant) for FRED as well as Pipeline as compared to the control and other neurovascular stents. The proportion of contrast transport governed by diffusion (diffusive amplitude) increased after implantation of Pipeline and FRED devices (Figure 6), with a corresponding decrease in convective amplitude.

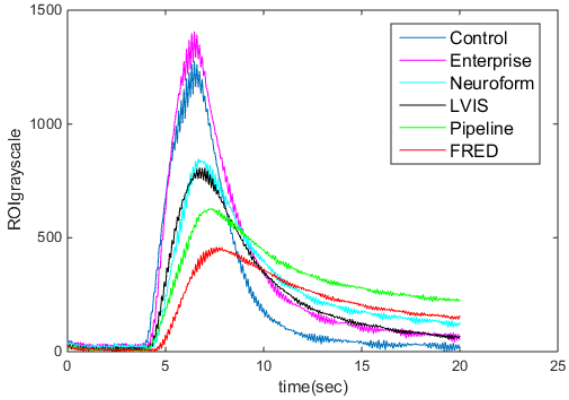

FIGURE 5: CONCENTRATION TIME CURVES FOR CONTROL MODEL WITHOUT ANY DEVICE AND THE FIVE MODELS WITH DEVICES

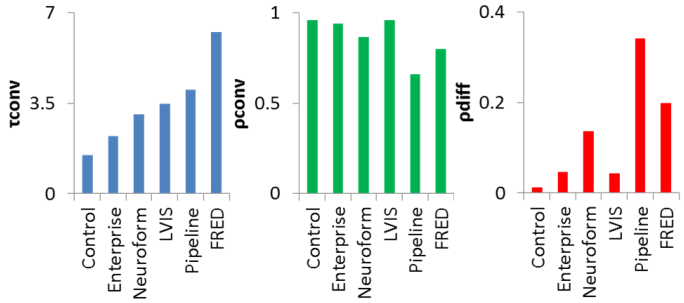

FIGURE 6: COMPARISON OF CONVECTIVE DECAY TIME CONSTANT, CONVECTIVE TRANSPORT AMPLITUDE, AND DIFFUSIVE TRANSPORT AMPLITUDE

Preliminary results show better performance of devices designed to be flow diverters. Following completion of microCT data based CFD analysis, we aim to correlate the angiographic parameters with the CFD parameters and compare device performance vis-à-vis implanted porosity and pore-density.

REFERENCES

1) Sadasivan C, et al., IEEE Transactions on Medical Imaging. 2009;28(7):1117-25
2) Y. Liu, et al., Engin. with Comp., 2012;28(4):305-318